High-Resolution Size-Discrimination of Single Nonionic Synthetic Polymers with a Highly Charged Biological Nanopore

Gerhard Baaken,[†,‡] Ibrahim Halimeh,[†,‡] Laurent Bacri,[§] Juan Pelta,[§] Abdelghani Oukhaled,[*,§] and Jan C. Behrends[*,†,∥,⊥]

[†]Laboratory for Membrane Physiology & -Technology, Department of Physiology, University of Freiburg, Hermann Herder Strasse 7, 79104 Freiburg, Germany, [‡]Ionera Technologies GmbH, Hermann Herder Strasse 7, 79104 Freiburg, Germany, [§]Laboratoire LAMBE, Équipe Polymères aux Interfaces, LAMBE UMR 8587 CNRS, Évry and Cergy University, Cergy-Pontoise 95011 cedex, France, [∥]Freiburg Materials Research Centre (FMF), University of Freiburg, Stefan-Meier-Strasse 21, 79104 Freiburg, Germany, and [⊥]Centre for Interactive Materials and Bioinspired Technologies (FIT), Georges-Köhler-Allee 105, 79110 Freiburg, Germany

ABSTRACT Electrophysiological studies of the interaction of polymers with pores formed by bacterial toxins (1) provide a window on single molecule interaction with proteins in real time, (2) report on the behavior of macromolecules in confinement, and (3) enable label-free single molecule sensing. Using pores formed by the staphylococcal toxin α-hemolysin (aHL), a particularly pertinent observation was that, under high salt conditions (3−4 M KCl), the current through the pore is blocked for periods of hundreds of microseconds to milliseconds by poly(ethylene glycol) (PEG) oligomers (degree of polymerization approximately 10−60). Notably, this block showed monomeric sensitivity on the degree of polymerization of individual oligomers, allowing the construction of size or mass spectra from the residual current values. Here, we show that the current through the pore formed by aerolysin (AeL) from *Aeromonas hydrophila* is also blocked by PEG but with drastic differences in the voltage-dependence of the interaction. In contrast to aHL, AeL strongly binds PEG at high transmembrane voltages. This fact, which is likely related to AeL's highly charged pore wall, allows discrimination of polymer sizes with particularly high resolution. Multiple applications are now conceivable with this pore to screen various nonionic or charged polymers.

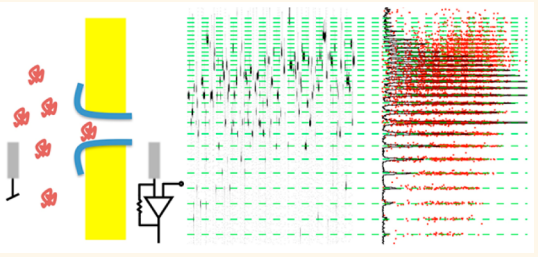

KEYWORDS: nanopore · ionic sensing · mass spectrometry · aerolysin · α-hemoylsin · poly(ethylene glycol)

Biological nanopores (mostly bacterial toxins and porins)[1,2] are used in ionic single molecule sensing and characterization following the resistive pulse principle, where the presence of an analyte inside the ion-conducting aqueous pore formed by the protein transiently reduces the current driven by a constant bias voltage, thus giving rise to a so-called resistive pulse. The most popular biological pore used for sensing to date is α-hemolysin (aHL) from *Staphylococcus aureus* which in its wild-type or various mutated forms interacts both with charged polymers such as nucleic acids[3] or synthetic polyelectrolytes[4,5] and with the nonionic polymer poly(ethylene glycol) (PEG).[6−10] One of the most intriguing phenomena observed in single-molecule sensing with α-hemolysin is the strong interaction of the pore with single PEG oligomers at high (3−4 M) salt concentrations that gives rise to long-lasting resistive pulses the amplitudes of which appear determined by the size or mass of the interacting PEG molecule.[11] As first shown by Kasianowicz, Krasilnikov and co-workers, the size-sensitivity of the conductance change is sufficiently great to enable nanopore-based single molecule mass spectrometry (Np-SMMS) with monomer resolution solely on the basis of electrical current recordings.[12] While it has been quantitatively described in terms of a simple model comprising a combination of size-exclusion and cation binding by PEG,[13,14] the mechanism of interaction underlying this mass discrimination by ionic current modulation is not fully

* Address correspondence to abdelghani.oukhaled@u-cergy.fr, jan.behrends@physiologie.uni-freiburg.de.

Received for review April 9, 2015 and accepted May 31, 2015.

Published online May 31, 2015
10.1021/acsnano.5b02096

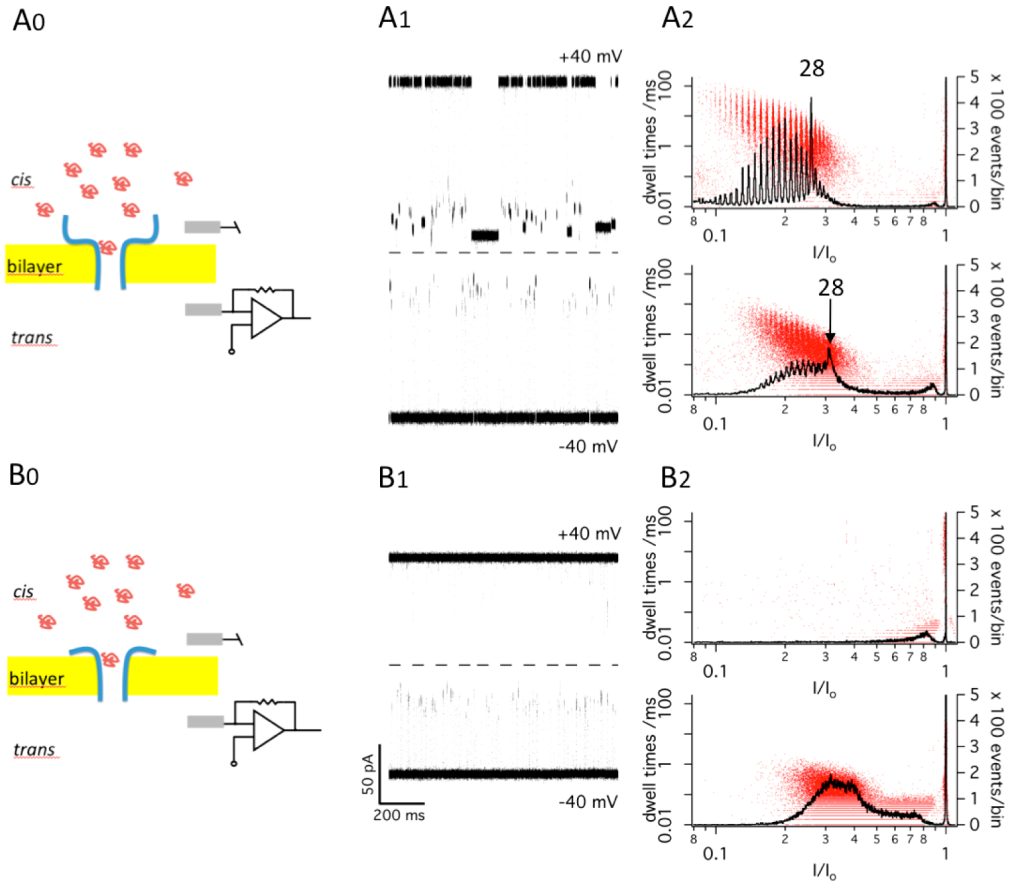

Figure 1. Interaction of polydisperse PEG of M_r = 1500) + monodisperse PEG 28 of M_r = 1251 (polyPEG1500 + monoPEG28) with aHL (A) and AeL (B). (A0 and B0) Schematics of the recording configuration. (A1 and B1) Superimposed traces (1s) for currents driven by *trans*-positive and *trans*-negative potentials (40 mV). Calibration in B applies to A equally. Dashed line is zero current. (A2 and B2) Histograms of relative residual conductance (I/I_o, black line) and superimposed scatterplots of dwell times plotted against I/I_o (red dots). Axes for I/I_o and dwell times are logarithmic.

understood. In particular, it is unknown to which extent this strong interaction, which for kinetic reasons must involve binding of the polymer to the pore wall,[1,12,13,15] is a unique property of aHL, or, indeed, whether it is at all shared by other pore-forming toxins. In general, possible differences between pore proteins in regard to interaction with PEG might yield important clues as to the precise mechanisms responsible for the exquisite size sensitivity observed.

Aerolysin (AeL) is a pore-forming toxin from *Aeromonas hydrophila*[16,17] that has also been used in sensing peptides,[18,19] proteins,[20−23] and sugars[24−26] but not to sense nonionic synthetic polymers. While the assembled aerolysin pore has not been amenable to X-ray crystallography, a combination of techniques has been used to predict its structural features to near-atomistic approximation.[27] In contrast to aHL, while also forming heptameric β-barrel pore assemblies, AeL does not possess a vestibule in its *cis*-domain (*i.e.*, the domain remaining extracellular upon insertion into a cell membrane), its general shape resembling more a rivet than a mushroom. In addition, unlike that of aHL, the AeL pore is thought to possess a high number (91) of charged residues pointing into its lumen.[27] The presence of these charges would be expected to give rise to pronounced ion selectivity and rectification. Indeed, aerolysin has been shown to be considerably more anion-selective and to display a lower total conductance than aHL.[28,29] Regarding binding of PEG, a highly charged pore wall might be expected to lead to weaker interaction following the general idea that PEG avoids charged species.[7,30]

We were interested in ascertaining, therefore, whether the nonionic polymer PEG would be detected by AeL and, if so, whether this interaction would equally show the strong size-dependence previously observed for the PEG/aHL system.

RESULTS AND DISCUSSION

The interaction of PEG with the aHL protein pore is known to be strongly enhanced by salt[7,11,15,31] and nanopore-based SMMS has been shown in the presence of 4 M[12,13,15,32,33] or 3 M KCl.[32,34,35]

Both the on-rate and duration of electrophysiologically detectable interactions between PEG and aHL are, in addition, dependent on transmembrane voltage,[13,15] with event durations (dwell times) being of particular importance for the precision with which

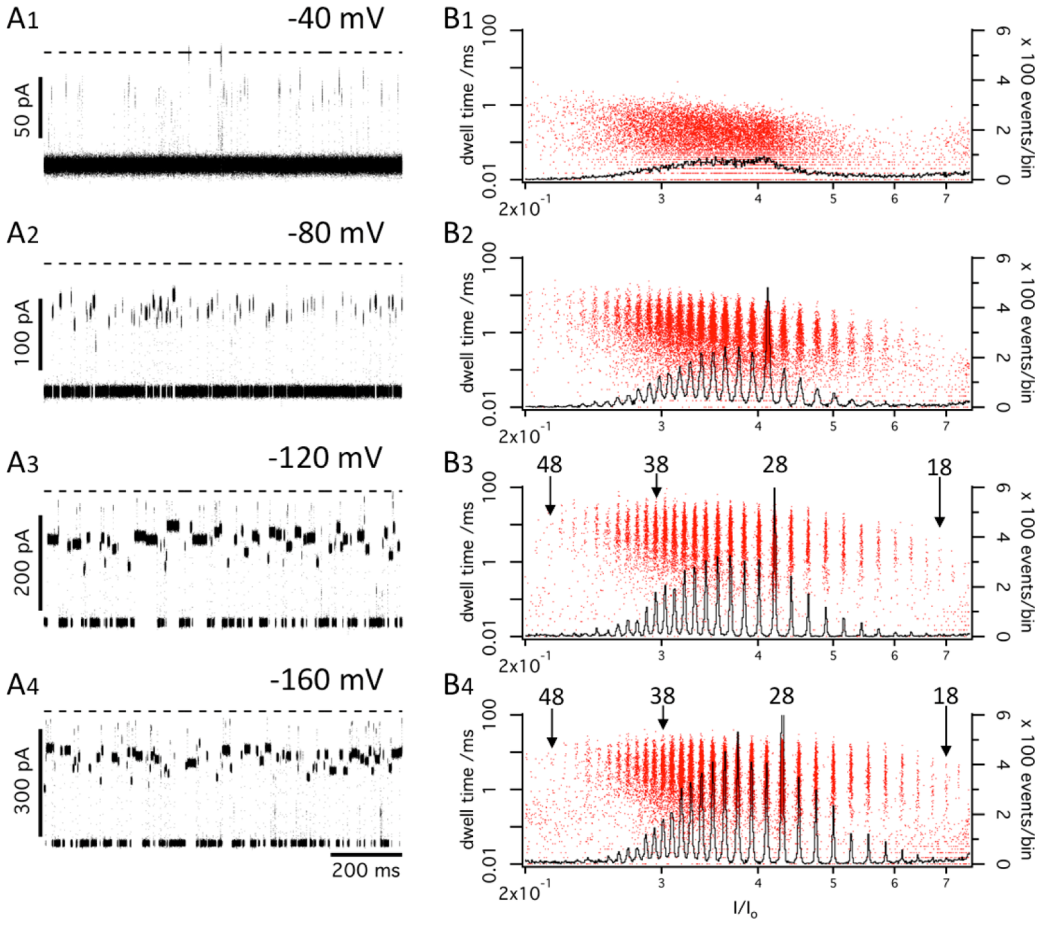

Figure 2. Interaction of polyPEG1500 + monoPEG28 with AeL at increasing *trans*-negative voltages. (A1−A4) The 1-s current traces as in Figure 1 at the applied voltages indicated. Note different calibrations of amplitude. (B) I/I_o histograms and scatterplots of dwell-time *vs* I/I_o corresponding to the recordings illustrated in)A) with axes as in Figure 1. For −120 and −160 mV, the positions of I/I_o-values for PEG of 18, 28, 38, and 48 r.u. are indicated.

the residual conductance can be determined by time-averaging the noisy current signal during each blocked state.[12] For the aHL/PEG system at 4 M KCl, the longest dwell times are observed at *trans*-positive voltages <50 mV, with a possible maximum at about +40 mV.[15] Because these long dwell times favor high-precision current measurements, the initial demonstrations of single-molecule detection of PEG[11] as well as of Np-SMMS were also done at this potential.[12]

We therefore decided to initially compare AeL with aHL in 4 M KCl at +40 mV trans, using polydisperse PEG (M_r = 1500, polyPEG1500) spiked with an excess of highly monodisperse PEG of 28 repeat units (r.u.) (PEG28, M_r = 1252) as an internal standard.[13,32] The polymer was applied to the *cis*-side of the pore.

As can be seen from Figure 1, while aHL performed as expected, showing well-resolvable resistive pulses yielding a histogram of relative residual conductances (I/I_o) with clearly discernible maxima corresponding to the different species of PEG present, aerolysin at +40 mV did not appear to interact with PEG at all. Interestingly, while reversing the direction of the electrical field aHL gave much shorter events and greatly reduced the quality of mass-resolution, it was precisely this reversal that in the case of AeL produced clear resistive pulses, albeit without discernible maxima in the I/I_o-histogram.

While increasing the voltage in the *trans*-positive direction did not produce an enhancement of PEG−AeL interaction (see also Figure 4), larger voltages applied in the *trans*-negative direction yielded the surprising result shown in Figure 2: At −80 mV, events clearly became longer and a series of maxima in the I/I_o-histogram appeared. A further prolongation of the mean dwell time of resistive pulses occurred at −120 mV, while at −160 mV, the mean dwell time for the events corresponding to PEG species larger than about PEG24 appear to decrease again (Figure 2B, see also Supporting Information Figure S2). It will be noted that the peak-to-valley ratio for the histogram obtained at −120 mV approaches 1, and compares favorably with that obtained with aHL at +40 mV under the same experimental conditions and using the same recording apparatus. In addition, maxima corresponding to PEG species between PEG17 and PEG47, *i.e.*, covering a mass range from M_r = 767 to 2088, can be discerned

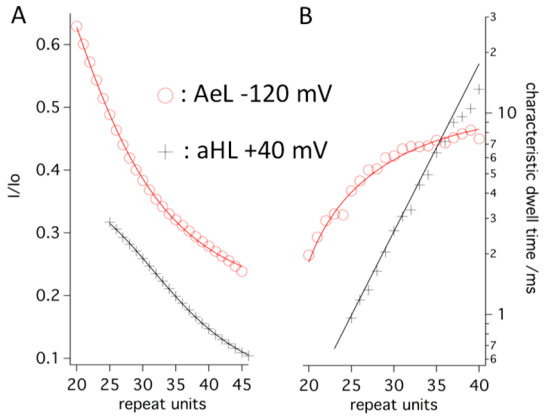

Figure 3. Comparison of the size-dependence of residual conductance (I/I_o, panel A) and characteristic dwell time (panel B) for aHL and AeL at +40 and −120 mV, respectively.

while at the optimal voltage for aHL (+40 mV *trans*), maxima from PEG24 to PEG48 were visible.

There are a number of reasons for this superior performance of AeL as a sensor especially for the smaller PEG species. First is the fact that well-defined and resolved resistive pulses can be measured at driving forces at least three times larger than with aHL, while background noise does increase by less than 16% (from 3.33 to 3.86 pA) r.m.s from −40 to −120 mV at the bandwidth used (0−20 kHz, 8-pole Bessel filter). Thus, signal-to-noise ratio increases by a factor of approximately 2.7. In addition, as shown in Figure 3A, the relationship between polymer number and I/I_o (size-conductance relation) has a steeper slope with AeL (0.028/r.u. *versus* 0.011/r.u. with aHL) for PEGs up to 30 r.u., explaining the very wide spacing between histogram maxima in this size range. However, the superior detection of small PEGs by AeL is probably mainly due to the long characteristic dwell times of events as compared to aHL over most of the mass range, as shown in Figure 3B. Dwell times for PEG species of one degree of polymerization are mono-exponentially distributed (see Supporting Information Figure S1) as previously shown for aHL.[12,13,32] However, the exponential decrease of the characteristic dwell times from PEG 40 to PEG20 seen for aHL is not present in the case of AeL. In fact, the dwell times of PEG binding events to the AeL pore show much less sensitivity to size in this mass range such that even for small PEGs (20−25 r.u,) they average >1 ms at −120 mV (Figures 2B and 3B). While in the case of aHL, even at the most favorable voltage of +40 mV these events last only for few hundreds of microseconds on average, and are therefore not fully resolved under the present recording conditions Figure 1A2 (see also refs 32, 34, 35 but see ref 33), the very well resolved events with AeL at −120 mV easily enable detection of PEGs of r.u. <20 at a bandwidth of 0−20 kHz from the present recordings.

In the experiments described above, PEG was present on the *cis* side of the membrane spanning

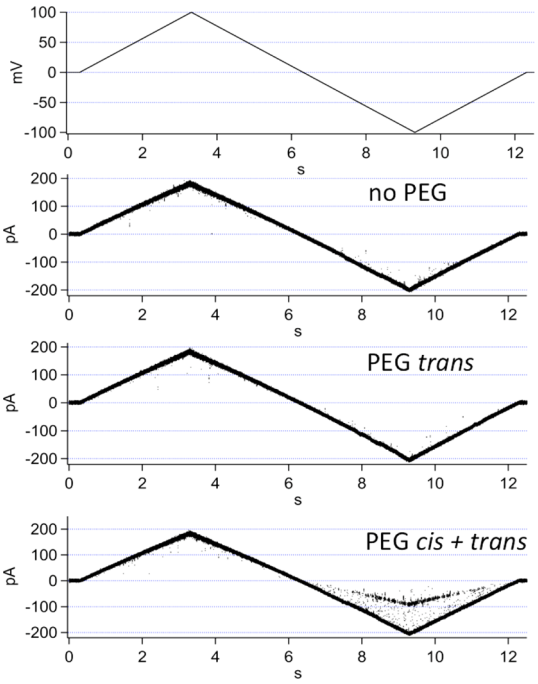

Figure 4. Interaction of polyPEG1500 with AeL during ramp-like variation of the *trans*−*cis* voltage between −100 and +100 mV (upper panel). Note the slight *trans*-ward rectification indicating physiological insertion of the AeL pore from the *cis*-compartment. The lower three panels show the corresponding current signals, with no PEG present, PEG present in the *trans*-compartment only, and PEG present in both compartments, respectively.

the microelectrode cavity. Under these conditions, interactions with AeL were only detectable at *trans*-negative but not *trans*-positive voltages.

Voltage-dependence of interaction between PEG and aHL has been ascribed to a positive charge acquired by the intrinsically neutral PEG due to the coordination of cations,[12,13,15,36] with the latest estimate based on molecular dynamics simulations having 1.5 K^+-ions bound on average to a PEG of 29 repeat units.[14]

While PEG coming from the compartment held at a negative potential binds to the aHL pore with lower on-rates than PEG added to the positive side,[15,32] this on rate is not zero, as observed here with PEG and AeL. In addition to acquired positive charge, one would, therefore, have to postulate a high energy barrier for entry of PEG from the *cis*-side of AeL that needs to be overcome by an electrophoretic force acting on PEG's acquired charge.

To test whether the need for an electrophoretic force promoting entry into the pore can explain our findings, we performed an experiment where PEG was first applied to the *trans*-side. If the voltage-dependence of interaction is determined through modulation of pore entry by an electrophoretic force, blocks by *trans*-side PEG should, conversely, be observed at *trans*-positive but not with *trans*-negative potentials. To do this, we used a classical bilayer setup

with two accessible chambers (see Methods). The AeL pore was inserted from the *cis*-side, and, as in all other experiments, its orientation checked by determining the IV-relation, which for physiologically oriented AeL (*i.e.*, stem pointing toward the *trans*-chamber) shows higher conductance for positive charges flowing from *cis* to *trans*, *i.e.*, *trans*-ward rectification, as opposed to aHL, which shows *cis*-ward rectification (see Figure S3 in Supporting Information). Surprisingly, as shown in Figure 4, when PEG is present on the *trans*-side of the AeL, pore blocks are observable neither at *trans*-positive nor at *trans*-negative voltages, while *cis*-side PEG shows clear blocks of the pore only with *trans*-negative potentials, corroborating the findings above. It is important to keep in mind that pore blocks by PEG observable by current recording require both entry of the polymer into the pore and binding, because without binding diffusion times would be on the order of nanoseconds and therefore not resolvable. With current methodology, there is no means to distinguish between entry and binding; we here use the term interaction to encompass both events.

Thus, while PEG's voltage-dependent interaction with AeL from the *cis*-side could be explained by the need for an electrophoretic force to overcome an energy barrier, the complete lack of interaction from the *trans*-side with potentials up to +100 mV is not in line with a dominant role of electrophoresis.

According to a recent quasi-atomistic structure model, the heptameric AeL pore contains a total of 91 charged residues (13 per monomer) facing the pore lumen.[27] Of these, 7 carry positive (lysin) and 6 have negative charge (glutamate or aspartate). Thus, the pore wall presents a net charge of +7. Importantly, two rings of positive charges are placed next to each other in the *trans*-ward third of the β barrel stem, while above and below negative and positive rings alternate.

A relative dominance of positive charges is in line with the mild anion-selectivity of the pore. Both the resulting enrichment of anions as counterions at the pore wall, as well as the greater anion permeability would mean that electroosmotic flow would be toward the positively charged compartment. Thus, electroosmotic force is unable to explain the voltage-dependence of the interaction observed here.

Regardless, the potential asymmetry found for PEG interaction with AeL is not likely to be explained by an acquired charge of PEG alone, but appears to be dominated by the structure and/or pore charges of AeL.

CONCLUSIONS

In summary, we find that PEG interaction with the AeL pore is in principle similar to but in important and potentially instructive ways different from its well-known interaction with the aHL pore. From an application point of view, which is the focus of the present report, Np-SMMS using AeL yields enhanced mass discrimination due to a combination of high signal-to-noise ratio as a consequence of the large driving force, a steeper mass-conductance relation and, most importantly, prolonged dwell times for smaller PEGs. Together, these features enable a very precise determination of residual conductance levels in the size range <PEG 25 where Np-SMMS with aHL requires exceptionally high-resolution, high-bandwidth recordings[13] and/or some form of *post-hoc* correction for limited bandwidth.[32,33,37]

Regarding our understanding of the basic physicochemical mechanism of interaction, our results strongly hint at a decisive role of the pore's geometrical and electrostatic properties. Especially, the new finding that for the same polymer under identical electrolyte conditions the voltage-dependence of dwell times is drastically different between two pores of the same family is highly significant. Current models, which interpret the voltage-dependence of nonionic polymer interaction with protein pores as a consequence of charges acquired by cation coordination,[13,14,36] may thus have to be revised to explain the strong increase of dwell times with *trans*-negative voltages observed for AeL. Further experimental and theoretical work is clearly needed to ascertain a possible role of AeL's highly charged pore in this context.

METHODS

Nanopore Recordings. Except for the experiments shown in Figure 4, bilayers were formed by remote liquid spreading[35] of diphytanoyl-phosphocholine (DPhPC, Avanti Lipids, Alabaster, AL) in octane (5 mg/mL) on a MECA-16 microelectrode cavity array chip[32,34,35,38] using the Orbit-16 automated parallel bilayer platform (Nanion Technologies, Munich, Germany) as described in detail in ref 35. Bilayer formation and pore insertion was controlled with the Orbit-16's internal multichannel patch-clamp amplifier (Triton-16, Tecella, Foothill Ranch, CA) running under TecellaLab (Vs. 0.84b) software. Current traces shown and analyzed were measured using an external Axopatch-200B patch clamp amplifier in capacitive feedback mode that could be switched between channels using the Orbit's internal probe selector controlled by OrbitControl software (Nanion). The signal was filtered at 100 kHz cutoff (4-pole Bessel filter integrated in the Axopatch) and subsequently at 20 kHz cutoff (8-pole Bessel filter, Model 9002, Frequency Devices, Ottawa, IL) and digitized at 200 kHz sampling rate using a NI-PCI6221 AD-converter (National Instruments, Austin, TX) running under GePulse software (Michael Pusch, University of Genova, Italy). All experiments were conducted in aqueous 4 M KCl solution buffered with 25 mM Tris and set to pH 7.5 with HCl. Electrolyte solutions were saturated with AgCl for enhanced stability of the microelectrode potential at high KCl concentrations. Stock solutions of PEG 1500 (Sigma-Aldrich, Schnelldorf, Germany) and PEG 28 (Polypure, Oslo, Norway) were prepared in 4 M KCl as above at a concentration of 10 mg/mL and added to the chamber to a final concentration of 0.33 mg/mL (PEG1500) and 0.033 mg/mL (PEG28). α-Hemolysin was purchased from

Sigma-Aldrich (Schnelldorf, Germany) and dissolved and stored in deionized water at a concentration of 0.17 mg/mL. Prior to an experiment, the stock solution was further diluted to a concentration of 8.5 μg/mL in 4 M KCl of which 3 μL was immediately added to the measurement chamber leading to a final concentration of 0.17 μg/mL. Pro-Aerolysin stock solution (0.178 mg/mL, kindly provided by Manuela Pastoriza-Gallego) was diluted 1:40 in DI water, activated by incubation with 9000 U/mL trypsin (Promega, Madison, WI) for 15 min at room temperature (23 °C) and subsequently stored on ice. For pore insertion, 4 μL was added to the measurement chamber to a final concentration of 0.12 μg/mL.

For the experiment shown in Figure 4, a classical vertical lipid bilayer setup (Warner Instruments, Hamden, CT) was used to allow continuous access to both sides of the membrane which was formed by manual painting from a DPhPC in decane (10 mg/mL) over a 150 μm wide aperture separating two compartments (*cis* and *trans*) The *cis* compartment was at ground. After thinning of the decane film and formation of a planar bilayer, the pores were formed by adding activated aerolysin (see above) from a 0.1 μg/mL stock solution to the 1 mL *cis* compartment. Single-channel currents were recorded with an Axopatch 200B patch-clamp amplifier (Molecular Devices, Sunnyvale, CA) in the whole-cell mode. Data were filtered using an 8-pole Bessel filter (the internal filter of the Axopatch 200B) at a cutoff frequency of 10 kHz and digitally acquired at 10 kHz sampling rate with a DigiData 1440A AD-converter running under Clampex 10 software (Molecular Devices) . All other experimental conditions were identical to those for the experiments shown in the other figures (see above).

Conflict of Interest: The authors declare the following competing financial interest(s): J.C.B. is a co-founder and shareholder of Ionera Technologies GmbH as well as of Nanion Technologies GmbH.

Acknowledgment. We thank Manuela Pastoriza-Gallego (Cergy) for providing pro-aerolysin, Ekaterina Zaitseva (Freiburg) for protein analysis and Sönke Petersen and Juan del Rio (Freiburg) for producing and testing the MECA chips. We are grateful to John J. Kasianowicz (Gaithersburg) for helpful discussions. This work was supported by grants from the Bundesministerium für Bildung und Forschung (BMBF, FKZ 0315316B, to J.C.B.) and the Bundesministerium für Wirtschaft und Technologie (BMWi, Exist Research Transfer, FKZ 03EFT9BW44, to G.B. and J.C.B.), the European Commission (Innovative Training Network 642083 "Eurosequences", to Ionera Technologies) the Deutsche Forschungsgemeinschaft (DFG, in the framework of the IRTG 1642 Soft Matter Sciences, to J.C.B.), the Agence Nationale de la Recherche (ANR 12-NANO-0012-03, to A.O.) and the Region Ile-de-France in the framework of DIM Nano-K (No. 094251, to A.O.).

Supporting Information Available: Details on the determination of characteristic dwell times from probability densities, the size dependence of dwell times at −60, −120, and −160 mV as well as on the rectification currents through aerolysin and α-hemolysin. The Supporting Information is available free of charge on the ACS Publications website at DOI: 10.1021/acsnano.5b02096.

REFERENCES AND NOTES

1. Kasianowicz, J. J.; Robertson, J. W. F.; Chan, E. R.; Reiner, J. E.; Stanford, V. M. Nanoscopic Porous Sensors. *Annu. Rev. Anal. Chem.* **2008**, *1*, 737–766.
2. Majd, S.; Yusko, E. C.; Billeh, Y. N.; Macrae, M. X.; Yang, J.; Mayer, M. Applications of Biological Pores in Nanomedicine, Sensing, and Nanoelectronics. *Curr. Opin. Biotechnol.* **2010**, *21*, 439–476.
3. Kasianowicz, J. J.; Brandin, E.; Branton, D.; Deamer, D. W. Characterization of Individual Polynucleotide Molecules Using a Membrane Channel. *Proc. Natl. Acad. Sci. U.S.A.* **1996**, *93*, 13770–13773.
4. Murphy, R. J.; Muthukumar, M. Threading Synthetic Polyelectrolytes through Protein Pores. *J. Chem. Phys.* **2007**, *126*, 051101-1–051101-4.
5. Jeon, B.-J.; Muthukumar, M. Determination of Molecular Weights in Polyelectrolyte Mixtures Using Polymer Translocation through a Protein Nanopore. *ACS Macro Lett.* **2014**, *3*, 911–915.
6. Bezrukov, S. M.; Kasianowicz, J. J. The Charge State of an Ion Channel Controls Neutral Polymer Entry into Its Pore. *Eur. Biophys. J.* **1997**, *26*, 471–476.
7. Merzlyak, P. G.; Yuldasheva, L. N.; Rodrigues, C. G.; Carneiro, C. M. M.; Krasilnikov, O. V.; Bezrukov, S. M. Polymeric Nonelectrolytes To Probe Pore Geometry: Application to the Alpha-Toxin Transmembrane Channel. *Biophys. J.* **1999**, *77*, 3023–3033.
8. Bezrukov, S. M.; Kasianowicz, J. J. Neutral Polymers in the Nanopores of Alamethicin and Alpha-Hemolysin. *Biol. Membr.* **2001**, *18*, 453–457.
9. Movileanu, L.; Bayley, H. Partitioning of a Polymer into a Nanoscopic Protein Pore Obeys a Simple Scaling Law. *Proc. Natl. Acad. Sci. U.S.A.* **2001**, *98*, 10137–10141.
10. Movileanu, L.; Cheley, S.; Bayley, H. Partitioning of Individual Flexible Polymers into a Nanoscopic Protein Pore. *Biophys. J.* **2003**, *85*, 897–910.
11. Krasilnikov, O. V.; Rodrigues, C.; Bezrukov, S. Single Polymer Molecules in a Protein Nanopore in the Limit of a Strong Polymer-Pore Attraction. *Phys. Rev. Lett.* **2006**, *97*, 018301.
12. Robertson, J. W. F.; Rodrigues, C. G.; Stanford, V. M.; Rubinson, K. A.; Krasilnikov, O. V.; Kasianowicz, J. J. Single-Molecule Mass Spectrometry in Solution Using a Solitary Nanopore. *Proc. Natl. Acad. Sci. U.S.A.* **2007**, *104*, 8207–8211.
13. Reiner, J. E.; Kasianowicz, J. J.; Nablo, B. J.; Robertson, J. W. F. Theory for Polymer Analysis Using Nanopore-Based Single-Molecule Mass Spectrometry. *Proc. Natl. Acad. Sci. U.S.A.* **2010**, *107*, 12080–12085.
14. Balijepalli, A.; Robertson, J. W. F.; Reiner, J. E.; Kasianowicz, J. J.; Pastor, R. W. Theory of Polymer-Nanopore Interactions Refined Using Molecular Dynamics Simulations. *J. Am. Chem. Soc.* **2013**, *135*, 7064–7072.
15. Rodrigues, C. G.; Machado, D. C.; Chevtchenko, S. F.; Krasilnikov, O. V. Mechanism of KCl Enhancement in Detection of Nonionic Polymers by Nanopore Sensors. *Biophys. J.* **2008**, *95*, 5186–5192.
16. Buckley, J. T.; Howard, S. P. Aerolysin from Aeromonas Hydrophila. *Methods Enzymol.* **1987**, *165*, 193–199.
17. Howard, S. P.; Garland, W. J.; Green, M. J.; Buckley, J. T. Nucleotide Sequence of the Gene for the Hole-Forming Toxin Aerolysin of Aeromonas Hydrophila. *J. Bacteriol.* **1987**, *169*, 2869–2871.
18. Stefureac, R.; Long, Y.-T.; Kraatz, H.-B.; Howard, P.; Lee, J. S. Transport of A-Helical Peptides through A-Hemolysin and Aerolysin Pores. *Biochemistry* **2006**, *45*, 9172–9179.
19. Wang, Y.; Montana, V.; Grubišić, V.; Stout, R. F., Jr.; Parpura, V.; Gu, L.-Q. Nanopore Sensing of Botulinum Toxin Type B by Discriminating an Enzymatically Cleaved Peptide from a Synaptic Protein Synaptobrevin 2 Derivative. *ACS Appl. Mater. Interfaces* **2015**, *7*, 184–192.
20. Pastoriza-Gallego, M.; Rabah, L.; Gibrat, G.; Thiebot, B.; van der Goot, F. G.; Auvray, L.; Betton, J.-M.; Pelta, J. Dynamics of Unfolded Protein Transport through an Aerolysin Pore. *J. Am. Chem. Soc.* **2011**, *133*, 2923–2931.
21. Merstorf, C.; Cressiot, B.; Pastoriza-Gallego, M.; Oukhaled, A.; Betton, J. M.; Auvray, L.; Pelta, J. Wild Type, Mutant Protein Unfolding and Phase Transition Detected by Single-Nanopore Recording. *ACS Chem. Biol.* **2012**, *7*, 652–658.
22. Payet, L.; Martinho, M.; Pastoriza-Gallego, M.; Betton, J.-M.; Auvray, L.; Pelta, J.; Mathé, J. Thermal Unfolding of Proteins Probed at the Single Molecule Level Using Nanopores. *Anal. Chem.* **2012**, *84*, 4071–4076.
23. Pastoriza-Gallego, M.; Breton, M.-F.; Discala, F.; Auvray, L.; Betton, J.-M.; Pelta, J. Evidence of Unfolded Protein Translocation through a Protein Nanopore. *ACS Nano* **2014**, *8*, 11350–11360.
24. Bacri, L.; Oukhaled, A.; Hémon, E.; Bassafoula, F. B.; Auvray, L.; Daniel, R. Discrimination of Neutral Oligosaccharides through a Nanopore. *Biochem. Biophys. Res. Commun.* **2011**, *412*, 561–564.

25. Fennouri, A.; Przybylski, C.; Pastoriza-Gallego, M.; Bacri, L.; Auvray, L.; Daniel, R. Single Molecule Detection of Glycosaminoglycan Hyaluronic Acid Oligosaccharides and Depolymerization Enzyme Activity Using a Protein Nanopore. *ACS Nano* **2012**, *6*, 9672–9678.
26. Fennouri, A.; Daniel, R.; Pastoriza-Gallego, M.; Auvray, L.; Pelta, J.; Bacri, L. Kinetics of Enzymatic Degradation of High Molecular Weight Polysaccharides through a Nanopore: Experiments and Data-Modeling. *Anal. Chem.* **2013**, *85*, 8488–8492.
27. Degiacomi, M. T.; Iacovache, I.; Pernot, L.; Chami, M.; Kudryashev, M.; Stahlberg, H.; van der Goot, F. G.; Dal Peraro, M. Molecular Assembly of the Aerolysin Pore Reveals a Swirling Membrane-Insertion Mechanism. *Nat. Chem. Biol.* **2013**, *9*, 623–629.
28. Wilmsen, H. U.; Pattus, F.; Buckley, J. T. Aerolysin, a Hemolysin from Aeromonas hydrophila, Forms Voltage-Gated Channels in Planar Lipid Bilayers. *J. Membr. Biol.* **1990**, *115*, 71–81.
29. Chakraborty, T.; Schmid, A.; Notermans, S.; Benz, R. Aerolysin of Aeromonas Sobria: Evidence for Formation of Ion-Permeable Channels and Comparison with Alpha-Toxin of Staphylococcus Aureus. *Infect. Immun.* **1990**, *58*, 2127–2132.
30. Lee, J. C.; Lee, L. L. Y. Preferential Solvent Interactions between Proteins and Polyethylene Glycols. *J. Biol. Chem.* **1981**, *256*, 625–631.
31. Bezrukov, S. M.; Vodyanoy, I.; Brutyan, R. A.; Kasianowicz, J. J. Dynamics and Free Energy of Polymers Partitioning into a Nanoscale Pore. *Macromolecules* **1996**, *29*, 8517–8522.
32. Baaken, G.; Ankri, N.; Schuler, A.-K.; Rühe, J.; Behrends, J. C. Nanopore-Based Single-Molecule Mass Spectrometry on a Lipid Membrane Microarray. *ACS Nano* **2011**, *5*, 8080–8088.
33. Balijepalli, A.; Ettedgui, J.; Cornio, A. T.; Robertson, J. W. F.; Cheung, K. P.; Kasianowicz, J. J.; Vaz, C. Quantifying Short-Lived Events in Multistate Ionic Current Measurements. *ACS Nano* **2014**, *8*, 1547–1553.
34. Zheng, T.; Baaken, G.; Vellinger, M.; Behrends, J. C.; Rühe, J. Generation of Chip Based Microelectrochemical Cell Arrays for Long-Term and High-Resolution Recording of Ionic Currents through Ion Channel Proteins. *Sens. Actuators, B* **2014**, *205*, 268–275.
35. del Rio Martinez, J. M.; Zaitseva, E.; Petersen, S.; Baaken, G.; Behrends, J. C. Automated Formation of Lipid Membrane Microarrays for Ionic Single-Molecule Sensing with Protein Nanopores. *Small* **2015**, *11*, 119–125.
36. Breton, M.-F.; Discala, F.; Bacri, L.; Foster, D.; Pelta, J.; Oukhaled, A. Exploration of Neutral *versus* Polyelectrolyte Behavior of Poly(ethylene glycol)s in Alkali Ion Solutions Using Single-Nanopore Recording. *J. Phys. Chem. Lett.* **2013**, *4*, 2202–2208.
37. Gu, Z.; Ying, Y.-L.; Cao, C.; He, P.; Long, Y.-T. Accurate Data Process for Nanopore Analysis. *Anal. Chem.* **2015**, *87*, 907–913.
38. Baaken, G.; Sondermann, M.; Schlemmer, C.; Rühe, J.; Behrends, J. C. Planar Microelectrode-Cavity Array for High-Resolution and Parallel Electrical Recording of Membrane Ionic Currents. *Lab Chip* **2008**, *8*, 938–944.